Analysis of Sections Subjected to Combined Shear and Torsion—A Theoretical Model

by Khaldoun N. Rahal and Michael P. Collins

A three-dimensional behavioral truss model capable of analyzing rectangular reinforced and prestressed concrete sections subjected to combined loading is presented. This model uses the principles of the modified compression field theory (MCFT), and is capable of analyzing sections subjected to combined biaxial bending, biaxial shear, torsion, and axial load. Compatibility of curvatures is introduced to enable the model to handle combined shear and torsion, and explain nonlinearity in the shear-torsion interaction curve. The model provides a check on spalling of the concrete cover for sections subjected to combined shear and torsion.

Calculated deformations and ultimate loads from the model are compared with experimental results and are shown to be in good agreement.

Many structural elements are subjected to load combinations that include significant torsion and shear. Fig. 1(a) and (b) show two examples: an elevated guideway structure, and a frame on the edge of a building or in a multideck bridge structure. In general, six actions may be acting on a section: torsion T, axial load N, vertical shear V_y, vertical bending M_y, lateral shear V_z, and lateral bending M_z [Fig. 1(c)].

The North American design provisions (ACI,[1] CSA[2]) for members subjected to combined loading are semi-empirical, and are incomplete, since they do not cover the case of the six combined actions. Moreover, ACI[1] provisions do not cover prestressed concrete members subjected to torsion. In addition, treatment of the issue of spalling of concrete cover is inconsistent with the Canadian code,[2] which assumes that, under torsion, the concrete cover will spall off, while ACI provisions account for a torsional contribution from the cover.

Engineers designing sections subjected to complex loading must sometimes supplement the code provisions with analytical models from the literature, such as that of Rabbat and Collins,[3] which was developed in 1975. However, these models often do not include the latest research findings, such as softening of the compressive strength of diagonally
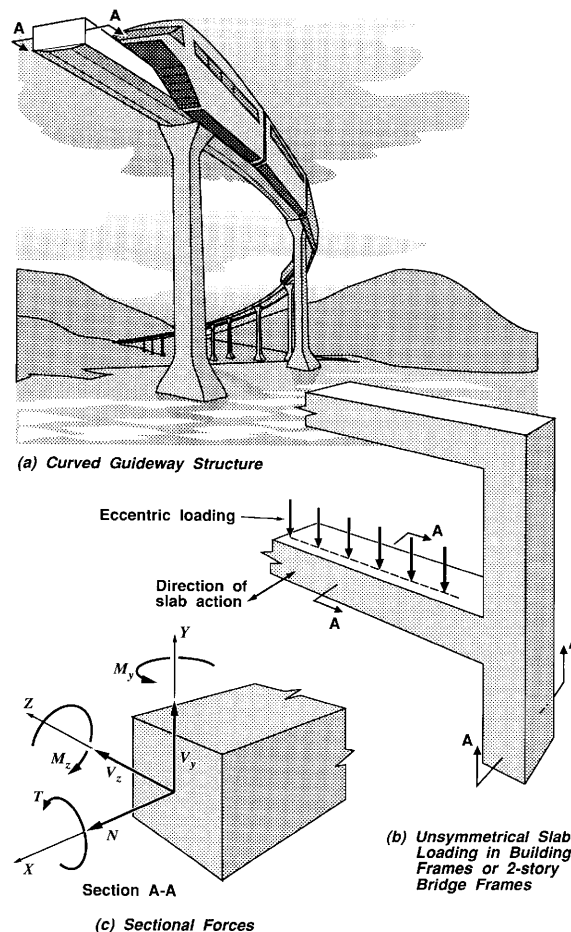

(a) Curved Guideway Structure

(b) Unsymmetrical Slab Loading in Building Frames or 2-story Bridge Frames

(c) Sectional Forces

Fig. 1—Examples of structures subjected to combined sectional forces

Khaldoun Najib Rahal *is a structural engineer with Morrison Hershfield Ltd. Consulting Engineers, Toronto, Ontario, Canada. Currently, he is involved in the design of the Hibernia Gravity Base Structure in St. John's Newfoundland. He holds degrees from the University of Toronto (1993), the University of Michigan at Ann Arbor (1987), and the American University of Beirut (1986).*

Michael P. Collins, FACI, is a professor in the Department of Civil Engineering at the University of Toronto. He is a member of joint ACI-ASCE Committee 445, Shear and Torsion, and ACI Committee 358, Concrete Guideways. He has acted as a consultant on the shear design of concrete offshore platforms.
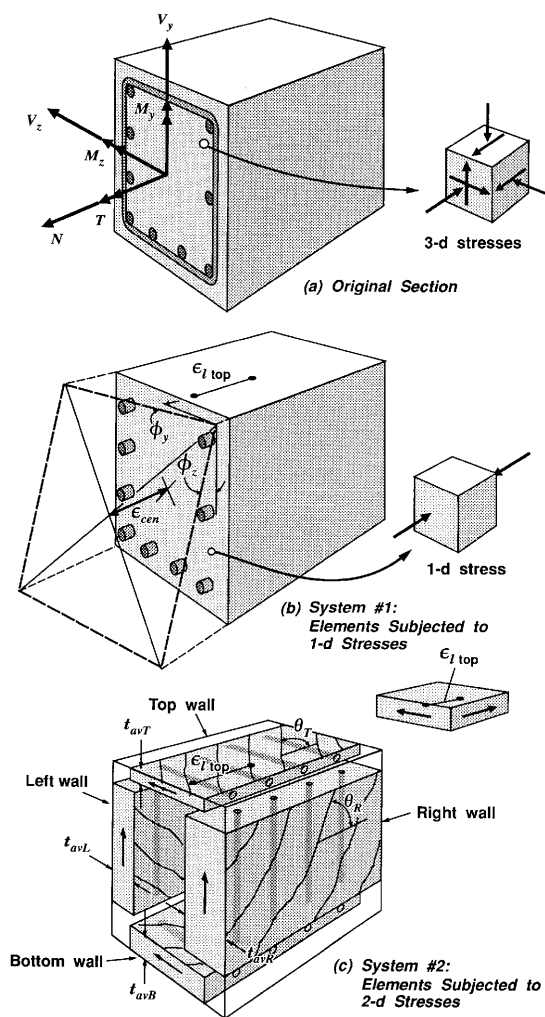
Fig. 2—Idealization of section

cracked concrete, the ability of cracked concrete to carry tension, and the ability of relatively small concrete covers to contribute to torsional and shearing resistance without spalling.

This paper presents an analytical model capable of predicting the behavior of reinforced concrete sections subjected to biaxial bending, biaxial shear, torsion, and axial load. The model considers the stress-strain relationship of cracked concrete and provides a direct check on spalling of concrete cover due to shear and/or torsion. It is believed that this model will be a contribution to the more rational analysis of reinforced concrete members subjected to complex loading.

DESCRIPTION OF THE MODEL

Fig. 2(a) (from Reference 4) shows the original section and three-dimensional stresses on a small element within the section. These stresses are complex, and cannot be determined easily with the current knowledge of cracked concrete behavior. To simplify the analysis, the section is idealized in such a way as to consider elements subjected to one- and two-dimensional stresses separately, while maintaining interaction between the two systems. Fig. 2(b) shows the idealized section resisting a portion of the applied actions (N, M_z, M_y, and the longitudinal stresses due to shear and torsion) by means of longitudinal stresses. As shown, the longitudinal strains are assumed to vary linearly over the section, i.e., plane sections remain plane, and the longitudinal stresses are related to the longitudinal strains by the usual uniaxial stress-strain relationships for the materials.

Fig. 2(c) shows the idealized section resisting torsion and shears (T, V_z, and V_y) by means of two-dimensional stresses. This section consists of four transversely reinforced walls with varying thickness and varying angle of principal compressive strains. Subscripts L, B, R, and T refer to the left, bottom, right, and top walls of the idealized section, respectively. Subscript i is used to refer to all four walls when a property or equation is common to all of them. The terms b and h are the sectional width and depth, respectively.

Interaction between Systems 1 and 2

Links between the two idealized systems are the longitudinal strains ε_l (obtained from System 1 and used in System 2) and longitudinal forces due to shear and torsion (obtained from System 2 and used in System 1). Hence, each wall is subjected to a shear force and a longitudinal strain ε_l . Equations of the modified compression field theory[5] can then be used to solve for the complete state of stress and strain in each wall.

A number of requirements must be satisfied within this model before the predicted response can be obtained. These requirements include:

1. Over the section: equilibrium of the shearing stresses (System 2) and longitudinal stresses (System 1), and compatibility of strains in the longitudinal direction (System 1).

2. In each wall: constitutive laws for steel and concrete (MCFT) (Systems 1 and 2); condition of compatibility of average strains (MCFT) (System 2); condition of equilibrium of average stresses (MCFT) (System 2); and compatibility of curvatures (System 2).

REQUIREMENTS OVER THE SECTION
Equilibrium of shearing stresses (System 2)

The four walls are tied together by the requirements of equilibrium of shearing stresses. It is assumed that V_y is resisted solely by the two vertical walls, while V_z is resisted solely by the horizontal walls.

Hence, the vertical shear stress v in the vertical walls can be related to V_y by

$$v = \frac{V_y}{b_v d_v} \tag{1}$$

(a) Strains **(b) Stresses** **(c) Stress Block** **(d) Location of Equivalent Force**
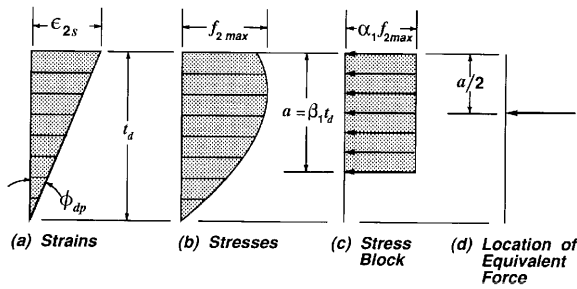
Fig. 3—Strain and stress distributions across wall thickness and equivalent stress block

where b_v and d_v are, respectively, the "web" width and effective flexural depth for vertical moment. Similarly, the horizontal shear stress v in the horizontal walls is related to V_z by

$$v = \frac{V_z}{b_v d_v} \tag{2}$$

where, now, b_v is the web width and d_v is the effective flexural depth for lateral moment. Note that b_v and d_v in Eq. (2) are different from those in Eq. (1).

The shear flow q circulating around the section provides the resistance to torque and hence

$$T = 2A_o q \tag{3}$$

where A_0 is the area enclosed by the shear flow.

Shearing stresses and principal compressive strains $_2$ will vary across the wall thickness t_d. Experimental evidence obtained by Mitchell and Collins[6] has shown that the diagonal compressive strains associated with shear flow vary linearly across the wall thickness. Fig. 3(a) and (b) show a linear distribution of strains, and the corresponding parabolic distribution of stresses, respectively. It is convenient to replace the parabolic stress distribution by an equivalent rectangular stress block, as is done in flexural calculations. Note that the depth of this equivalent stress block is called a.

The shear stress τ due to applied torque, and acting across a thickness a, is given by

$$\tau = \frac{q}{a_i} = \frac{T}{2A_o a_i} \tag{4}$$

where a is the equivalent thickness of the diagonal, effective in resisting torsion. [Fig. 3(c)]. The area enclosed by the shear flow can be related to a_i, b, and h, the dimensions of the section, by the following relationship

$$A_o\left(b - \frac{a_L}{2} - \frac{a_R}{2}\right)\left(h - \frac{a_T}{2} - \frac{a_B}{2}\right) \tag{5}$$

For the critical wall, where τ and v are additive, the shear stress distribution is assumed to be as shown in Fig. 4(a). The

uniform shear stress due to the shear force acts over a thickness t_{sh}, and is computed using Eq. (1) and (2), with t_{sh} taken as half the effective shear width. The equivalent uniform shear stresses due to torsion act over a width a_i of the wall and are calculated by Eq. (4).

The modified compression field theory for shear developed by Vecchio and Collins[5] has been successfully used in membrane elements and beams. To apply this theory to the present model, an average value v_{av} of the shearing stress shown in Fig. 4(a), acting on an appropriate thickness t_{av}, must be computed. The terms t_{av} and v_{av} shown in Fig. 4(a) are calculated in such a way as to provide a shear loading equivalent to the original system of stresses. Averaging τ and v across t_{av} underestimates the concrete compressive stresses in the outer fiber of the wall, ε_{2s}. A special check, described later, is conducted to calculate the maximum concrete compressive stress, which is the indicator of crushing of concrete.

Equilibrium of longitudinal stresses (System 1)

The longitudinal stresses in the section must be in equilibrium with the applied axial force and biaxial moment. Since torsion and shearing forces cause additional longitudinal stresses in the section, their contribution must also be taken into account.

The concrete and steel stresses (obtained from strain distribution over the section, and using the material constitutive laws), when integrated over the section, should add up to the sectional forces. Hence

$$\int_{A_c} f_c dA_c + \int_{A_p} f_p dA_p = N + \sum_{i=1}^{4} N_{vi} \tag{6a}$$

$$\int_{A_c} f_c y\, dA_c + \int_{A_s} f_s y\, dA_s + \int_{A_p} f_p y\, dA_p = -M_z - \sum_{i=1}^{4}(y_i N_{vi}) \tag{6b}$$

$$\int_{A_c} f_c z\, dA_c + \int_{A_s} f_s z\, dA_s + \int_{A_p} f_p z\, dA_p = -M_y - \sum_{i=1}^{4}(z_i N_{vi}) \tag{6c}$$

where A_c, A_s, and A_p are, respectively, the areas of concrete, nonprestressed steel, and prestressed steel in the section, and f_c, f_s, and f_p are, respectively, the stresses in the concrete, nonprestressed steel, and prestressed steel. z_i and y_i are, respectively, the z- and y-coordinates of the centroid of Wall i. The right-hand sides of these equations are the total equivalent actions, which are the summation of the applied loads and those due to the effect of shearing stresses. N_v is the longitudinal force due to wall shearing stresses, and is computed for each of the walls using the following equation

$$N_{vi} = \left(\frac{v_{avi}}{\tan\theta_i} - f_{1i}\right) \tag{7}$$

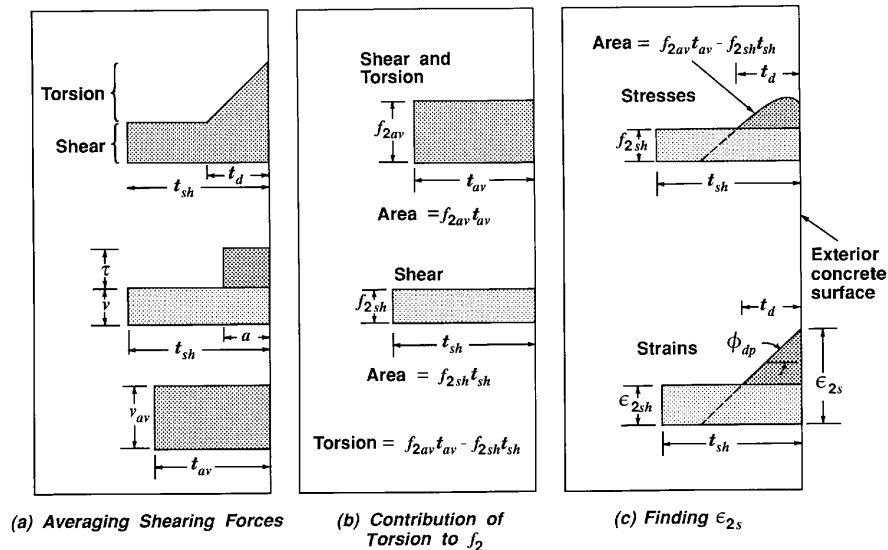where f_1 is the average tensile stress in diagonally cracked concrete.

Fig. 4—Averaging wall stresses and finding 2s

Compatibility of longitudinal strains (System 1)

Fig. 2(b) shows a general view of the deformation of the section in the longitudinal direction. The section may be curved in both the horizontal and vertical planes. Three independent variables are necessary to describe the state of longitudinal strain and, consequently, the state of longitudinal stress. Fig. 2(b) shows the variables chosen for this model, along with their sign convention. These variables are:

ε_{cen} = longitudinal strain at section centroid, taken positive if tensile

ϕ_z = curvature about z-axis, taken positive if it causes compression in top fiber

ϕ_y = curvature about y-axis, taken positive if it causes compression in right fiber

For a given combination of ε_{cen}, ϕ_z, and ϕ_y, longitudinal strain ε_l at any point with coordinates (y, z) can be computed as follows:

$$\varepsilon_l = (\varepsilon_{cen} - y\phi_z + z\phi_y) \tag{8}$$

The model assumes a perfect bond between the concrete and steel. Hence, Eq. (8) can be used to compute strain in the concrete and in reinforcing bars at the section. The strain in the prestressed steel is that in the concrete plus $\Delta\varepsilon_p$, the strain difference between the tendon and surrounding concrete, which depends on the specifics of the prestressing operation.

REQUIREMENTS WITHIN THE WALLS

The constitutive laws, and compatibility and equilibrium requirements incorporated in the modified compression field theory (MCFT), are satisfied, and compatibility of curvatures between the walls is also insured.

Compatibility of curvatures (System 2)

In each wall, the twist ψ of the section, longitudinal curvature ϕ_l, transverse curvature ϕ_p, and maximum curvature (along θ) ϕ_{dp} are related by the requirement of compatibility. The following equation can then be deduced[7]

$$\phi_{dp} = \phi_l \sin^2(\theta) + \phi_l \cos^2(\theta) + \Psi \sin(2\theta) \tag{9}$$

Care should be taken with the signs of the longitudinal and transverse curvatures. For example, the transverse curvature in the right wall is computed using the following equation

$$\phi_{t-R} = \frac{\varepsilon_{t-L} - \varepsilon_{t-R}}{b_o} \tag{10}$$

where b_0 is the center-to-center dimension of the vertical leg of the stirrups. The transverse curvature in the left wall will be of opposite sign to that in the right wall.

Given ϕ_{dp} and the strain at the surface ε_{2s}, the thickness of the diagonal is computed by

$$t_d = \frac{\varepsilon_{2s}}{\phi_{dp}} \tag{11}$$

Concrete surface strains (System 2)

The compressive strain at the surface of concrete ε_{2s} is an indicator of crushing, which is a key aspect of the behavior of partially and completely over-reinforced sections. The analysis, which is based on the average values, v_{av} and t_{av} (Analysis 1), assumes a constant ε_2, and, hence, does not reflect the way ε_2 and τ change across the width of the wall. A special analysis is required to more accurately estimate ε_{2s}. This special analysis (Analysis 2) is based on the assumption that the principal compressive strains caused by torsion vary linearly across the width of the wall.

The values of f_{2av}, θ, and f_{2max} are obtained from Analysis 1. The combined shear and torsion contribution to concrete principal compressive stresses is $f_{2av} t_{av}$. The shear contribution is $f_{2sh} t_{sh}$, where f_{2sh} is

$$f_{2sh} = v_{sh}(\tan\theta + \cot\theta) - f_1 \tag{12}$$

The torsion contribution to the principal compressive stresses is, therefore, $f_{2av} t_{sh} - f_{sh} t_{sh}$. This contribution is used to calculate, by trial and error, the value of ε_{2s}, based on the assumption that ε_2 due to torsion varies linearly across t_d. [Fig. 4(c)]. The solution technique should consider the pos-

sibility that t_d may be greater than the wall thickness t. This case corresponds to partial plastification of the wall.

A numerical example in Reference 4 illustrates this check, carried out on the critical wall of the section of contraflexure of RC2-1 (Reference 4) tested under combined shear and torsion. The average value of ε_2 was 0.000174, while the surface strain ε_{2s} was 0.000294.

ε_{2s}, α_1, and β_1 are used to check for crushing of the concrete at the surface, and to update the values of A_0, and hence, better estimate the twist. Crushing is assumed to take place when the surface principal compressive strain ε_{2s} reaches 1.5 ε'_c.

SPALLING OF CONCRETE COVER

Fig. 5(a) shows the corners of a section subjected to torsion. The compressive stresses, which contribute to the resistance to applied torque, change direction near the corners. This creates tensile stresses in the direction perpendicular to the compressive stress direction. When the concrete cannot resist these tensile stresses, splitting takes place, usually along the weak plane formed by the transverse bars. Similar spalling can occur under shear or combined shear and torsion.

The mechanics of spalling have still not been adequately studied. However, since concrete cover is held to the section by the ability of concrete to resist tension, counting on the load carried in the cover is equivalent to relying on tensile stresses in the concrete.

Factors that increase the risk of spalling include:

1. Increasing the concrete cover.

2. Increasing f_2 (which may vary across the cover if torque is applied).

3. Increasing the area of steel at the interface between concrete inside and outside the stirrups.

4. Decreasing the tensile strength of concrete.

A measure of the weakening effect of the steel in the splitting plane may be given by

$$K_1 = \frac{\Sigma d_{bl} s + d_{bt}\rho_t}{\rho_t s} \tag{13}$$

where d_{bl} is the diameter of longitudinal bar, and the summation is taken over all the bars in contact with the stirrups. d_{bt} is the diameter of the stirrup bars, s is the spacing of the stirrups, and p_t is the perimeter of the stirrup. K_1 is approximately the ratio of the area occupied by the reinforcing bars to the total area along the perimeter of the stirrups.

The suggested measure of the potential of spalling in the vertical walls is given by

$$K_2 = \frac{K_1 \int f_2 d(z)}{\sqrt{f_c'} b_v} \tag{14a}$$

Integration is carried out along the clear cover only. For the horizontal walls, integration is performed in the direction of y, and b_v is replaced by d_v. Assuming that $\sqrt{f_c'}$ is proportional to the tensile strength and that it carries the units of stress, the coefficient K_2 is dimensionless.
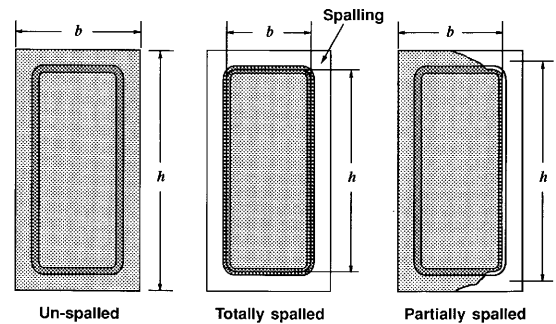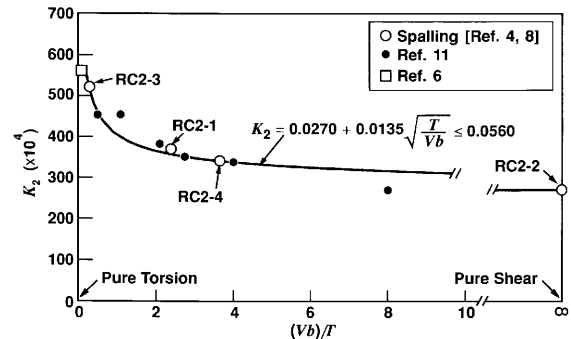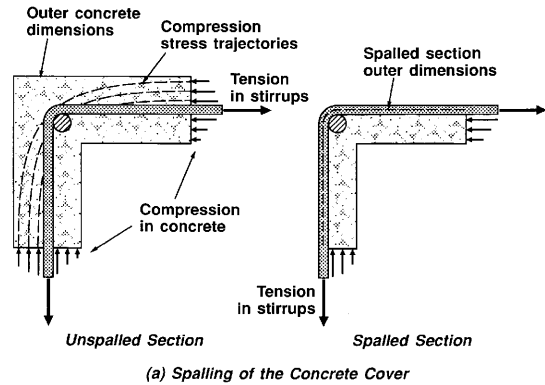

(a) Spalling of the Concrete Cover

(b) Calculated K_2 for Shear and Torsion Tests

(c) Effect of Spalling on Section Dimensions

Fig. 5—*Spalling in section*

K_2-values (at loads at which spalling was observed or at ultimate loads, whichever takes place first) were analytically computed for the specimens subjected to shear and torsion, from References 4, 6, and 10 [Fig. 5(b)]. A measure of K_2 at which spalling was first detected (based mostly on specimens of Series 2 of Rahal and Collins[8]) is given by

$$K_3 = 0.0270 + 0.0135 \sqrt{\frac{T}{Vb}} \le 0.0560 \tag{14b}$$

where the value of $T/(Vb)$ is positive. The factor K_3 is dimensionless.

To insure that the spalling load is always greater than the cracking load, and to avoid very conservative predictions for spalling in sections with large thickness of concrete cover, spalling is assumed to take place only if ε_{2s} exceeds 20 percent of ε'_c.

Reduction in dimensions due to spalling

From the literature on tests on combined shear and torsion that reported whether or not spalling occurred before the ul-
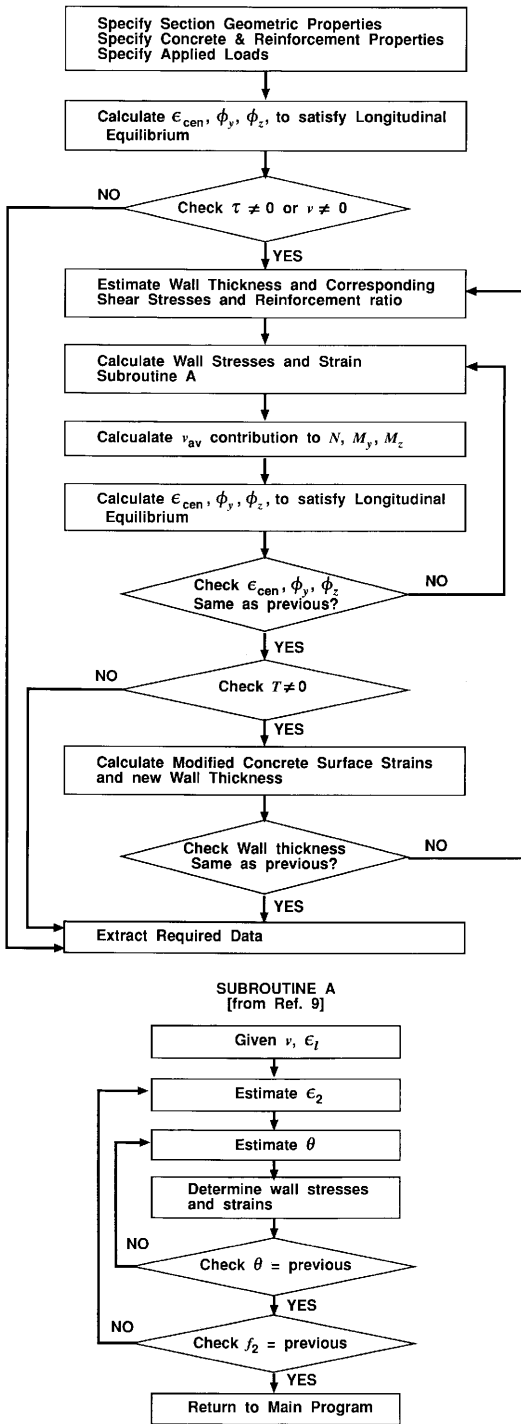
SUBROUTINE A
[from Ref. 9]

Fig. 6—Flow chart of analysis computer program COM-BINED

timate capacity was reached (primarily Reference 8), the following can be concluded:

Case 1—In the case of high $T/(Vb)$, the magnitudes of ($\tau + v$), τ , and ($\tau - v$) may all be large enough to cause spalling, and, hence, spalling can affect the cover around the whole section.

Case 2—In the case of small $T/(Vb)$, the magnitude of ($v + \tau$) and ($v - \tau$) are both large enough to cause spalling, which affects the shear width, providing most of the resistance to shear.

Case 3—When the ratio is neither considerably large nor small, ($\tau - v$) does not cause spalling while ($\tau + v$) does. The other sides of the section are subjected to τ, usually not enough to cause spalling [depending on $T/(Vb)$]. These sides are, however, partially affected by spalling on the corners adjacent to the critical side ($\tau + v$).

Consequently, spalled dimensions depend on the torque-shear ratio. With only a limited number of tests on spalling of sections subjected to combined shear and torsion, the recommended values of the dimensions b and h to be used in analysis are conservative [Fig. 5(c)]. They apply under the following limitations:

1. Fig. 5(c.1) for the case of no spalling.

2. Fig. 5(c.2) for the case of severe spalling, occurring under the following conditions

$$\frac{T}{Vb} \le \frac{1}{5} \ \text{ or } \ \frac{T}{Vb} \ge 5 \qquad (15)$$

3. Figure 5(c.3) for the case of partial spalling, affecting one side of the section fully, and the two adjacent sides partially, and occurring under the following conditions

$$\frac{1}{5} < \frac{T}{Vb} < 5 \qquad (16)$$

In this case, assuming that only half the cover is spalled is a conservative choice.

APPLICATIONS OF THE MODEL

The equations of this model were implemented into a computer program, COMBINED, which is based on the algorithm shown in Fig. 6.

The model is based on the MCFT, which has proved to be a good tool for analyzing the behavior of sections subjected to combined shear, bending, and axial load. In this paper, the reliability of the model is verified by comparing calculations of the model with experimental results from tests on pure torsion, shear, and combined shear and torsion. Special emphasis is given to the prediction of spalling. The comparison is divided into two parts: calculating deformations, and calculating ultimate loads and interaction diagrams.

Predicting deformations

An advantage of the present model is that it allows the full load-deformation response (up to ultimate capacity) of a section under combined loading to be calculated. This includes calculating the steel and concrete strains, as well as the overall sectional deformations, such as twist, elongation, and curvatures. The model also calculates cracking loads and checks the mode of failure.

To check the applicability of torsion and spalling assumptions adopted in the model, the response of two specimens loaded in pure torsion was calculated. Specimen PT5 (Reference 6) had essentially no cover, while Specimen PT6 (Reference 6) had a 40-mm-thick cover. Fig. 7 compares the calculated and observed response, including twist, and the transverse, longitudinal, and principal compressive strains. Very good agreement is observed. Of special interest, the calculated concrete compressive strains compared very well
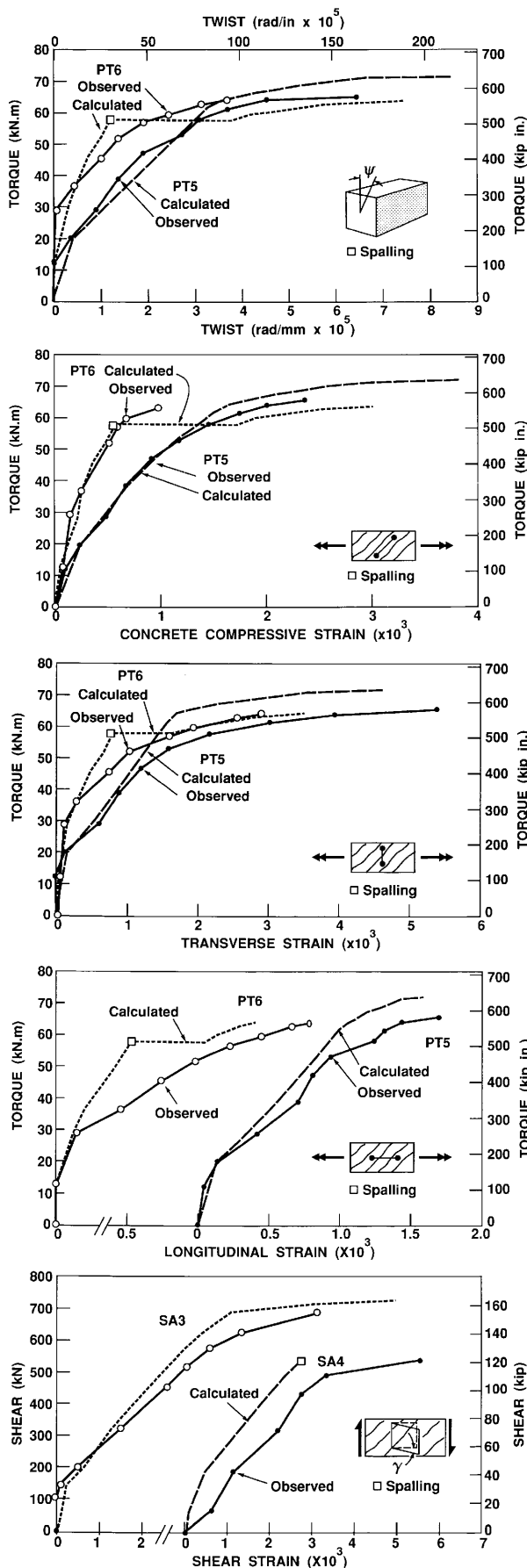
Fig. 7—Comparison between calculated and measured load-deformation curves of University of Toronto tests on pure torsion[6] and shear[9]

with the observed strains. The results of the model show good agreement with those from the tests in both cases, when spalling takes place and when it does not.

The validity of applying the spalling check to sections subjected to shear and to combined shear and torsion is checked here with the use of experimental data from Arbesman,[9] and Rahal and Collins.[8]

Specimen SA3 (Reference 9) (no cover on the vertical sides) did not suffer from spalling, while SA49 (Reference 9) (cover = 40 mm on the vertical sides) did. Fig. 7 shows the calculated and measured shear strain. It should to be noted that SA3 and SA4 were test regions in the same specimen, and that test region SA4 was preloaded when SA3 was tested. This explains the relatively large observed deformations in SA4.

Fig. 8 compares the calculated and observed response of seven specimens tested by Rahal and Collins.[8] The three specimens of Series 1, shown in Fig. 8(a), had a clear cover of 23 mm, while the four specimens of Series 2, shown in Fig. 8(b), had a clear cover of 43 mm. Deformations shown in Fig. 8 include transverse strains, twist, and lateral curvatures. Of special interest is the ability of the model to capture the lateral curvature in sections subjected to shear and torsion [Fig. 8(d)]. The shearing stresses on the side where τ and v are additive are larger than those where τ and v are subtractive. Larger shearing stresses cause larger longitudinal stresses and strains. The different longitudinal strains cause the lateral curvature.

The specimens of Series 1 were predicted to remain unspalled, while those of Series 2 were predicted to spall considerably, reducing their stiffness and strength.

The accuracy of the model in calculating deformations and capturing the effects of spalling of the concrete cover is evident from the results illustrated in Fig. 7 and 8.

Predicting ultimate loads and interaction diagrams

The ability of program COMBINED to calculate accurately shear-torsion interaction diagrams was checked by using experimental data from References 8 and 10 through 13. Fig. 9 shows calculated and observed interaction diagrams for tests by Rahal and Collins[8] (Series 2), where spalling affected the ultimate loads, and Klus,[10] Pritchard,[12] and Ewida and Mc-Mullen.[13] Very good agreement was observed. Table 1 summarizes the correlation of the calculations of COMBINED with experimental capacities of beams subjected to "pure" and "combined" torsion and shear. The average value of the ratio of observed to calculated load is 1.0, and the coefficient of variation is about 8 percent.

Curvature of *T-V* interaction diagrams

It can be seen from Fig. 9 that the observed shear strength-torsional strength interaction relationship consists of a convex curve rather than the straight lines that would result from a straight addition of torsional shear stress and "shear" shear stress. The reason for this nonlinearity is not well explained in the literature, but it is generally believed that it may be due to some "redistribution" of shearing stresses or "plastification" in the section.

In 1968, Klus[10] suggested that an increase in the percentage of transverse steel will increase the curvature of the *T-V*
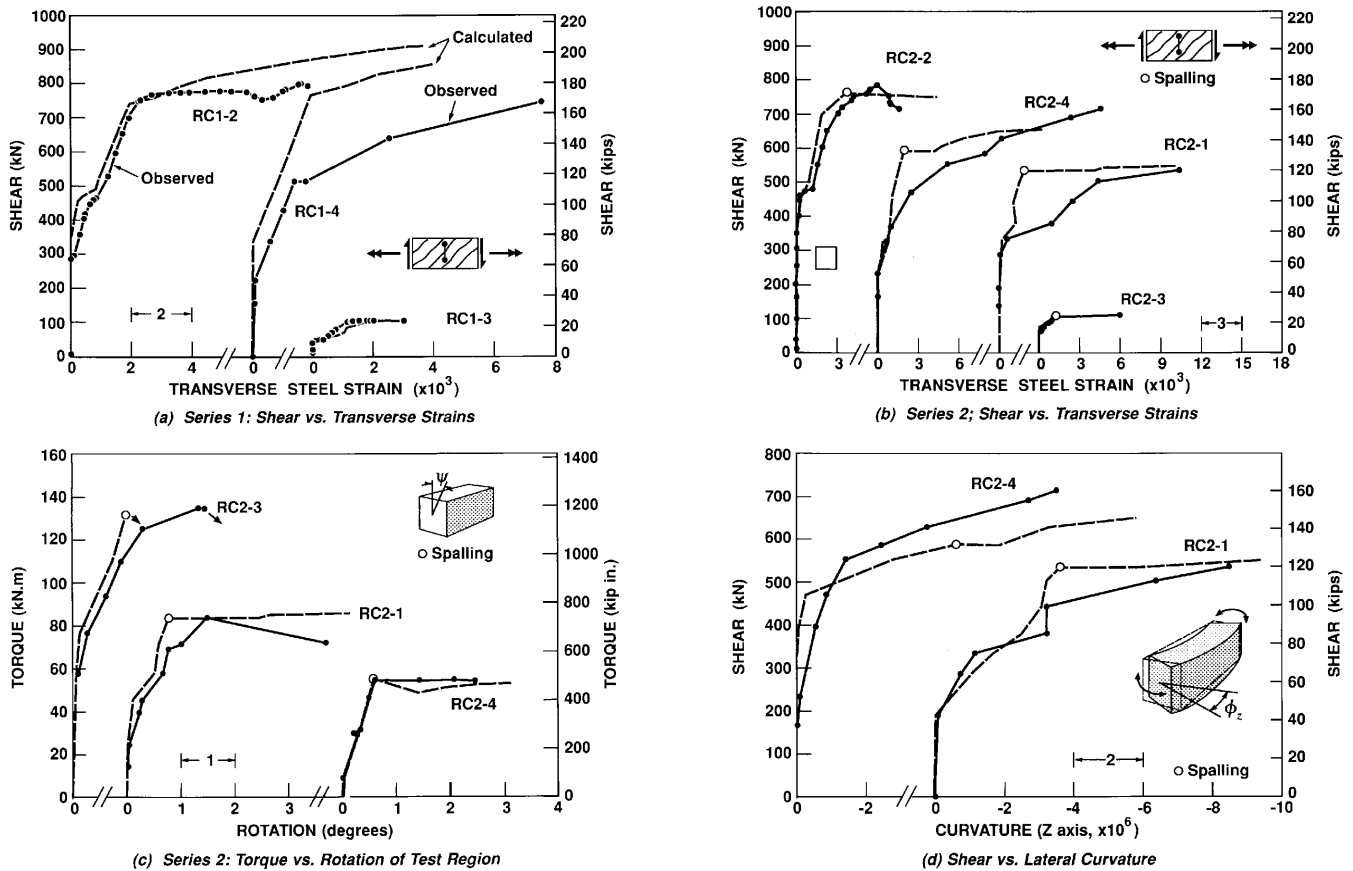
Fig. 8—Comparison between calculated and measured load-deformation curves of University of Toronto Tests[4,8] on combined shear and torsion

interaction diagram. In 1981, Ewida and McMullen[13] proved experimentally and theoretically that an increase in the amount of reinforcement increases the curvature of the interaction diagram. They recommended three different equations for the interaction of fully over-reinforced, partially under-reinforced, and under-reinforced sections. Ewida and McMullen[13] also showed that a small shear force can increase the torsional strength of heavily reinforced sections. They explained this increase by stating that "the failure is due to failure of the concrete in the compression zone. When a small shear force is applied, the compressive stresses are decreased (relieved) and the shear strength is thus enhanced. This phenomenon will be referred to as 'shear relief.'"[13]

The model presented in this paper makes use of the requirement of compatibility of curvatures to explain the curvature of the interaction diagram and increase in torsional strength when a relatively small shear force is applied. Fig. 10(a) shows the normalized interaction diagrams for three sections: under-reinforced, partially under-reinforced, and over-reinforced. Spalling was not a factor in this analysis. Note that very large amounts of reinforcement were used to insure that reinforcement did not yield (in the completely over-reinforced section), and magnify the curvature of the curves. Fig. 10(b) shows how the calculated average thickness t_{av} of the critical wall changed from the case of pure shear to that of pure torsion. The fact that the change in t_{av} is not linear confirms the idea of "redistribution." Eq. (9) and (11) provide an explanation. Applying proper sign conven-

tion to the terms of Eq. (9) indicates that, in the critical side of the section, the curvature in the longitudinal and transverse directions opposes that due to twist (along θ, ϕ_l, and ϕ_t cause tension while ψ causes compression). Eq. (11) indicates that decreasing or limiting ϕ_{dp} implies a larger value of t_d (and consequently t_{av}). Engaging a larger area of concrete in resistance "relieves" the concrete at the surface where crushing is expected, and confirms the idea of "redistribution." Considerable redistribution on hollow sections may cause partial "plastification" of the section.

Fig. 10(b) also shows that redistribution, and consequently the curvature of the interaction diagram, are more significant in heavily reinforced sections. It also shows that increasing the amount of steel increases the thickness of the equivalent tube resisting pure torsion. This was noted by Mitchell and Collins.[6] Their equation for t_d showed that an increase in the amount of reinforcement increases the force that the reinforcement can carry, and, consequently, requires an increase in the thickness t_d of the equivalent hollow tube of concrete that resists the applied torque. The same phenomenon takes place when the torque is combined with a shear force. The increase of the thickness t_d is to redistribute the stresses over a greater thickness of the wall. In hollow sections, the thickness t_d may become so large that redistribution almost causes "plastification" of the section. Fig. 10(b) shows plastification of the critical wall of the section with partially and fully over-reinforced sections.

Table 1—Correlation of the calculations of Program COMBINED with shear and torsin tests.

Specim	T_{exp}	V_{exp}	T_{calc}	V_{calc}	Ratio	Average	Coefficient of variation
Rahal and Collins [4,8]							
RC1-2	—	805	—	911	0.88	0.90	1.4%
RC1-3	140	107	153.	115.	0.91		
RC1-4	11	764	11.3	856	0.89		
RC2-1	83.5	535	85.6	548	0.98	1.03	3.9%
RC2-2	—	796	—	763	1.04		
RC2-3	135	111	131.	109	1.03		
RC2-4	57.6	715	52.9	657	1.09		
Klus [10]							
1, 2	—	157.	—	142.	1.11	1.03	4.5%
10	3.3	132.	3.26	130.	1.01		
6	5.88	117.	5.86	117	1.00		
9	7.4	101	7.43	101.	1.00		
5	8.82	93	8.42	88.8	1.05		
7	11.6	63.2	10.5	57.3	1.10		
8	12.5	30.8	12.7	31.3	0.98		
3, 4	14.7	—	14.7	—	1.00		
Badawy et al. [11]							
S5	—	151.	—	147.	1.03	1.08	3.0%
S6	8.9	93.4	8.1	84.5	1.11		
S7	11.6	48.9	10.5	44.3	1.10		
S2	13.5	—	12.7	—	1.06		
Pritchard [12]							
10	—	108.	—	126.	0.86	0.91	5.1%
9	5.97	87.7	6.41	94.2	0.93		
8	9.1	63.8	9.45	66.0	0.96		
7	11.1	39.5	11.7	41.3	0.96		
6	11.8	1.65	13.8	1.93	0.85		
Ewida and McMullen [13]							
P-1	12.1	—	13.6	—	0.89	1.01	9.2%
P-2	10.8	42.7	11.5	45.2	0.94		
P-3	9.0	70.8	9.0	70.6	1.00		
P-4	7.0	113.	6.33	102.	1.11		
P-5	—	149	—	131.	1.13		
Mitchell and Collins [6]							
PT5	65.3	—	73.0	—	0.89		
PT6	64.7	—	65.5	—	0.99		
Arbesman [9]							
SA3	—	729	—	700	1.04		
SA4	—	533.	—	520	1.03		
Average					1.00		
Coefficient of variable (percent)					7.8%		

Spalling is another factor that may increase the curvature of the *T-V* interaction diagram. Experiments[8] showed that sections subjected to relatively high or relatively low *T/V* may be severely affected by spalling, while sections subjected to intermediate values of *T/V* are only partially affected by spalling. This increases the curvature of the interaction diagram, since the reduction in area at intermediate *T/V* values is not as dramatic as that at extreme *T/V* values. The relative-

ly small calculated pure torsional capacity of specimens of Series 2[4,8] [Fig. 9(a)] provides such an example.

CONCLUSIONS

An analytical model has been developed capable of predicting the load-deformation response of rectangular reinforced concrete sections subjected to complex combinations of loads, including biaxial bending, biaxial shear, torsion, and axial load. The model, based on modified compression

(a) Tests by Rahal and Collins [Ref. 4, 8]

(b) Tests by Klus [Ref. 11]

(c) Tests by Pritchard [Ref. 13]
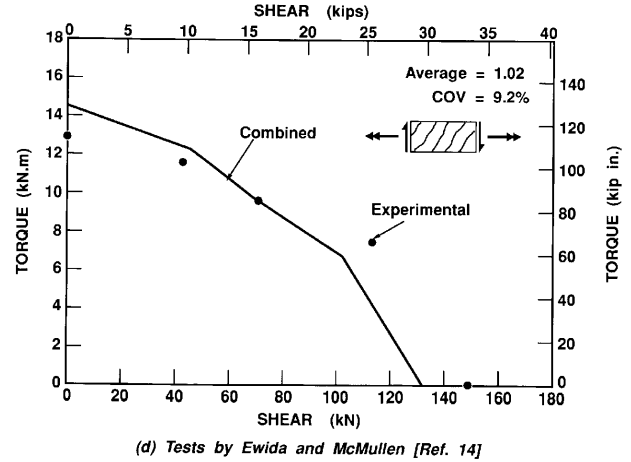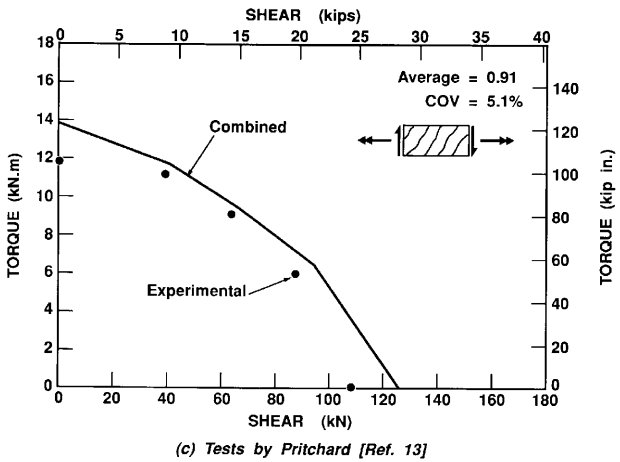
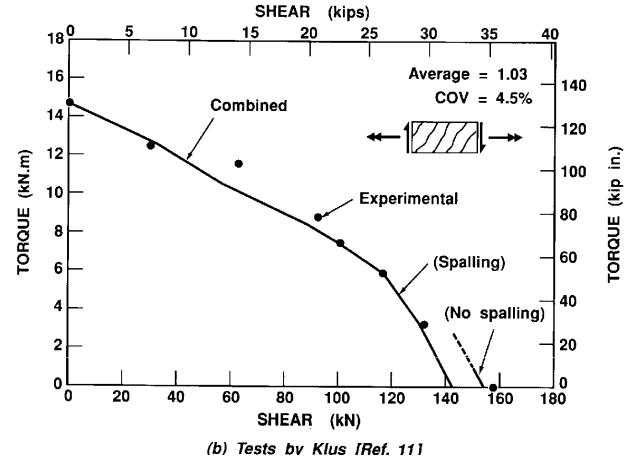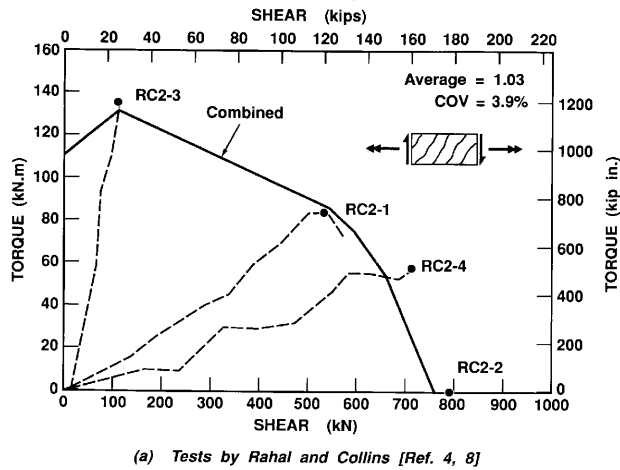(d) Tests by Ewida and McMullen [Ref. 14]

Fig. 9—Comparison between calculated and measured shear-torsion interaction diagrams

(a) Normalized T-V interaction Diagrams

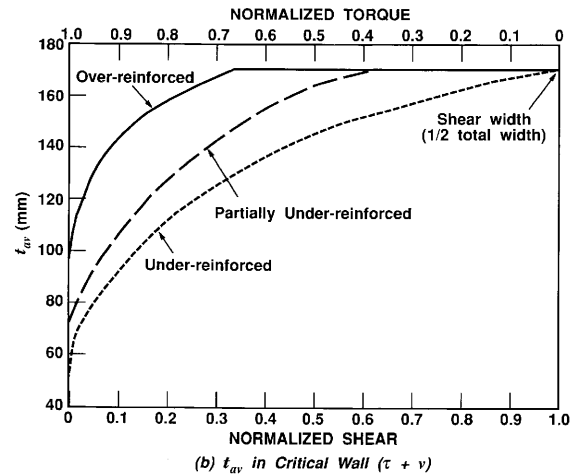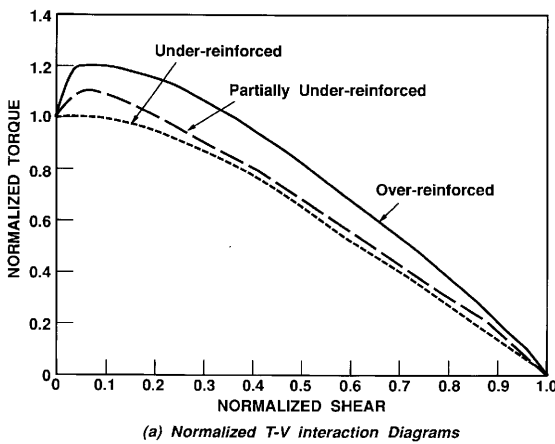(b) t_{av} in Critical Wall $(\tau + v)$

Fig. 10—V-T and V-t_{av} diagrams

field theory, considers the requirements of compatibility and equilibrium, and uses realistic constitutive laws.

Comparisons of calculations of the model with experimental results from members loaded in shear and/or torsion have shown that the model is a powerful tool for calculating the full response of sections subjected to combined loading.

Some of the features of the model are:

1. It allows ultimate loads and the full response of the section (up to ultimate loads) to be calculated.

2. It takes into account tensile stresses in cracked concrete, which enhances the accuracy of the calculated deformations.

3. It calculates cracking loads.

4. It determines steel and concrete strains, which enables the mode of failure of the section to be identified.

5. Effect of torsion on the distribution of concrete surface strains is estimated.

6. The possibility of spalling of the concrete cover is checked.

7. It accounts for softening of the concrete strength, which yields greater accuracy in the prediction of failure of over-reinforced sections.

8. It gives a rational explanation for the curvature in the shear-torsion interaction diagram based on the generally believed idea of "redistribution" of shearing stresses over the section. The model also shows that increasing the thickness of the concrete cover or amount of reinforcement adds to the curvature of the shear-torsion interaction diagram.

NOTATION

a	=	depth of equivalent stress block
A_0	=	area enclosed by shear flow
A_c	=	area of concrete of section
A_p	=	area of longitudinal prestressed steel
A_s	=	area of longitudinal nonprestressed steel
b	=	horizontal dimension of section
b_0	=	centrer-to-center distance between vertical legs of stirrups
b_v	=	shear width
d_{bl}	=	diameter of longitudinal reinforcing bar
d_{bt}	=	diameter of stirrup reinforcing bar
d_v	=	shear depth
f_c'	=	compressive cylinder strength of concrete
f_1	=	average concrete principal tensile stress
f	=	average concrete principal compressive stress
f_{2av}	=	average concrete principal compressive stress (due to shear and torsion)
f_{2sh}	=	concrete principal compressive stress due to shear force
f_{2max}	=	peak compressive strength of diagonally cracked concrete

a	=	depth of equivalent stress block
f_c	=	compressive stress in concrete
f_p	=	stress in prestressed steel
f_s	=	stress in nonprestressed steel
h	=	vertical dimension of section
K_1	=	spalling constant
K_2	=	spalling constant
K_3	=	spalling constant
M	=	bending moment about y-axis
M_z	=	bending moment about z-axis
N	=	axial force
p_t	=	perimeter of stirrup
q	=	shear flow
s	=	center-to-center spacing of stirrups
T	=	torsional moment
t_{av}	=	average wall thickness
T_{calc}	=	calculated torsional strength
t_d	=	thickness of diagonal compressive field under torsion
T_{exp}	=	observed torsional strength
T_s	=	steel contribution to torsional strength
t_{sh}	=	thickness of wall resisting shear

a	=	depth of equivalent stress block
v	=	shear stress
V	=	shear force
v_{av}	=	average combined shear stress
v_{sh}	=	shear stress due to shear force
V_y	=	shear force along y-axis
V_z	=	shear force along z-axis
x	=	coordinate along x-axis
y	=	coordinate along y-axis
z	=	coordinate along z-axis
α_1	=	stress factor in equivalent stress block
β_1	=	depth factor in equivalent stress block
ε	=	strain at peak strength of concrete cylinder
ε_2	=	principal compressive strain
ε_{2av}	=	average principal compressive strain due to shear and torsion
ε_{2s}	=	principal compressive strain at surface of concrete
ε_{2sh}	=	principal compressive strain due to pure shear
ε_{cen}	=	longitudinal strain at centroid of section
ε_l	=	average longitudinal strain
ε_t	=	average transverse strain
ϕ_{dp}	=	wall curvature in direction of θ
ϕ_l	=	wall curvature in longitudinal direction
ϕ_t	=	wall curvature in transverse direction
ϕ_y	=	sectional curvature in y-direction
ϕ_z	=	sectional curvature in z-direction
γ	=	shear strain in wall
Ψ	=	twist of section
θ	=	direction of plane of principal strain with respect to longitudinal axis
ε	=	shearing stress due to torsion
$\delta\varepsilon_p$	=	strain difference due to prestressing

REFERENCES

ACI Committee 318, "Building Code Requirements for Reinforced Concrete (ACI 318-89)," American Concrete Institute, Detroit, 1989, 353 pp.

2. CSA Committee A23.3, "Design of Concrete Structures for Buildings (CAN3-A23.3-M84)," Canadian Standards Association, Rexdale, 1984, 281 pp.

3. Rabbat, B., and Collins, M.P., "Variable Angle Space Truss Model for Structural Concrete Members Subjected to Complex Loading," *Douglas McHenry International Symposium on Concrete and Concrete Structures,* SP-55, American Concrete Institute, Detroit, 1978, pp. 547-587.

4. Rahal, K. N., "Behaviour of Reinforced Concrete Beams Subjected to Combined Shear and Torsion," PhD thesis, University of Toronto, 1993.

5. Vecchio, F. J., and Collins, M. P., "Modified Compression Field Theory for Concrete Elements Subjected to Shear," ACI JOURNAL *Proceedings* V. 83, No. 2, Mar.-Apr. 1986, pp. 219-231.

6. Mitchell, D., and Collins, M.P., "Behaviour of Structural Concrete Beams in Pure Torsion," *Publication* 74-06, Department of Civil Engineering, University of Toronto, 1974, 88 pp.

7. Onsongo, W. M., "Diagonal Compression Field Theory for Reinforced Concrete Beams Subjected to Combined Torsion, Flexure, and Axial Load," PhD thesis, University of Toronto, 1978, 246 pp.

8. Rahal, K. N., and Collins, M. P., "Effect of the Thickness of Concrete Cover on the Shear-Torsion Interaction—An Experimental Investigation," *ACI Structural Journal,* V. 92, No. 3, May-June 1995, pp. 334-342.

9. Arbesman, B., "Effect of Stirrup Cover and Amount of Reinforcement on Shear Capacity of Reinforced Concrete Beams," MEng thesis, University of Toronto, 1975, 176 pp.

10. Klus, J., "Ultimate Strength of Reinforced Concrete Beams in Combined Torsion and Shear," ACI JOURNAL, *Proceedings* V. 65, No. 3, Mar. 1968, pp. 210-216.

11. Badawy, H. E. I.; McMullen, A. E.; and Jordaan, I. J., "Experimental Investigation of the Collapse of Reinforced Concrete Curved Beams," *Magazine of Concrete Research,* V. 29, No. 99, June 1977, pp. 59-69.

12. Pritchard, R. G., "Torsion Shear Interaction of Reinforced Concrete Beams," MSc thesis, University of Calgary, 1970.

13. Ewida, A. A., and McMullen, A. E., "Torsion-Shear Interaction in Reinforced Concrete Members," *Magazine of Concrete Research,* V. 23, No. 115, June 1981, pp. 113-122.

14. Vecchio, F. J., and Collins, M. P., "Response of Reinforced Concrete to In-Plane Shear and Normal Stresses," *Publication* No. 82-03, University of Toronto, Mar. 1982, 332 pp.